Inherent Performance Limitations of Power-Autonomous Fuel Cell System

Kyung-Won Suh and Anna G. Stefanopoulou

***Abstract*— The performance and robustness of power-autonomous fuel cell operation depends on balance-of-plant controls, for instance, reactant flow, water and temperature management from it's own power. Transient performance in fuel cell power delivery is highly associated with air supply control among those. We present here inherent design limitations on autonomous operation of PEM fuel cells with compressor-driven air supply. To this end, we model and analyze the dynamics of a fuel cell system equipped with a compressor driven by the fuel cell itself. The analysis results clarify fundamental performance limitations in regulating oxygen delivery into the cathode. Several control architectures are proposed to demonstrate these limitations analytically and with simulations.**

***Index Terms*— Fuel cells, power systems, linear control, feedback control, bandwidth limitation, non-minimum phase system**

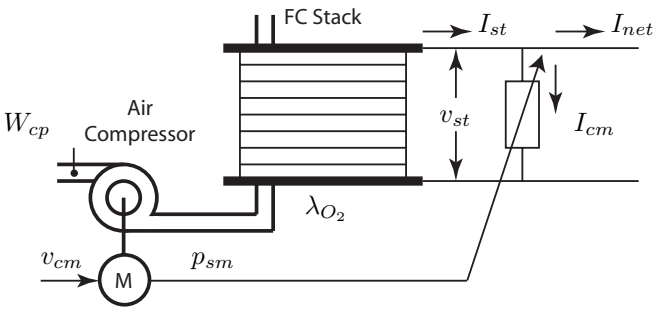

Fig. 1. Power-autonomous FC stack system

I. Introduction

The importance of the air delivery system in proton exchange membrane (PEM) fuel cell (FC) is widely recognized with several limitations on air supply control repeatedly reported in [1], [2], [3], [4]. For example, fuel cells, when operating with low gas flows to minimize parasitic losses, are prone to partial oxidant starvation during dynamic load changes even with optimized flow field design. The temporarily low oxidant stoichiometry produces cell voltage drop, resulting in local temperature increase. Anomalous operating conditions can cause not only reversible performance decrease but irreversible degradation [5], [6].

The oxygen is supplied through the air supply and it is typically achieved with a blower or a compressor. Although the compressor absorbs a significant amount of power and increases the fuel cell parasitic losses, it is preferred to a blower due to the resulting high power density (kW/m^3). A blower is typically not capable of pushing high flow rates through small channels; thus the blower requires large channel volumes, and thus larger stacks. Note here that there have been many studies analyzing the tradeoff between FC power density and parasitic losses from the air supply device [7]. Comparison of the dynamic flow capabilities of a FC system with a blower and a compressor can be found in [8]. It is shown that the two systems are dynamically similar in providing air flow in the cathode channels. The blower spends time spinning its rotor inertia, which is typically bigger than the compressor inertia, whereas the compressor spends time pushing the air and elevating the supply manifold pressure to significantly higher operating pressures than the ones in a blower supply.

The tradeoff between satisfying net power requirements and maintaining optimum oxygen excess ratio in the stack during load step changes is first defined in [9]. We show here the the limitations discussed in [9] are more critical when the compressor motor draws its power directly from the fuel cell in the case of an autonomous fuel cell operation. The limitations are analyzed based on a low order fuel cell model in Sec. II and Appendix I. In Sec. III, we discuss two feedforward control construction architectures (I_{st}-based and I_{net}-based) and compare them analytically and with simulation. Feedback control bandwidth limitations are clarified in Sec. IV. Finally, a proportional integral (PI) controller is used in Sec. V to demonstrate the bandwidth limitations that the compressor power coupling introduces to the oxygen regulation problem.

II. Power-autonomous operation of FC system

In high pressure PEM fuel cell system, a compressor supplies the air flow necessary for the reaction associated with the current drawn, I_{st} from the fuel cell as shown in Fig. 1. For several reasons [9], [10], the air supplied to the cathode should exceed the air necessary for reaction. The oxygen excess ratio λ_{O_2} (see Eq. (17) in Appendix) is a convenient lumped variable, which if regulated to a desired value ($\lambda_{O_2}^{ref} = 2$) ensures adequate supply of oxygen in the fuel cell stack.

In this study, we focus on the dynamic behavior and the air flow control problem of a power-autonomous fuel cell stack system. The problem is directly associated with the electrical and flow coupling between the compressor and the fuel cell stack. We consider here the case where the compressor is driven from the fuel cell, which is shown in Fig. 1. The total

This work is funded by NSF 0201332 and the Automotive Research Center (ARC) under U.S. Army contract DAAE07-98-3-0022.

K.-W. Suh and A. G. Stefanopoulou are with the Department of Mechanical Engineering, University of Michigan, Ann Arbor, MI 48109, USA kwsuh,annastef@umich.edu

current drawn from the fuel cell stack, I_{st} is defined by the net current I_{net}, which is the current from the FC to the load, and is augmented by the current load drawn from the all of the FC auxiliaries and particularly the compressor load, I_{cm}

$$I_{st} = I_{net} + I_{cm}. \tag{1}$$

Here it is considered that the compressor motor contributes to the largest percent of FC parasitic losses through the current drawn I_{cm} directly from the stack bus[1]. To calculate the current consumed by the compressor, we assume that the compressor motor has an ideal power transformer. The transformer supplies the necessary power P_{cm} dictated by the DC motor control signal v_{cm} in (18) by drawing a current I_{cm} at the FC stack bus voltage v_{st}

$$I_{cm} = P_{cm}/v_{st}. \tag{2}$$

The FC stack voltage v_{st} is given by the polarization curve in [3], [9]. Thus the compressor motor current is implemented so that P_{cm} is simply drawn from the stack through a DC motor control unit instantaneously.

The control objective of regulating performance variable λ_{O_2} can be achieved by a combination of feedback and feedforward algorithms that automatically define the compressor motor voltage input v_{cm}. Since the oxygen excess ratio λ_{O_2} is not directly measured, we control λ_{O_2} indirectly by measuring the compressor flow W_{cp} and the demanded load. Fig. 2 shows the feedback and feedforward controllers which are designed to regulate the oxygen excess ratio in power-autonomous fuel cell stack system. For results on control of the air flow and the system pressure using a compressor and a back throttle, see [4].

Regulating air flow based on the flow rate measurement at the supply manifold inlet has a potential limitation because the actual air flow at the cathode inlet is not the same as that at the compressor outlet, thus causing significant lag or delay on regulating oxygen excess ratio inside the stack [1], [3], [4]. On the other hand, high compressor control effort to overcome the limitation above can cause instabilities when the compressor draws current directly from the stack [2]. In the following sections, we will clarify and quantify these limitations and suggest possible solution to maximize performance within the limitations.

III. Feedforward control design

A feedforward controller is an obvious choice for oxygen excess ratio λ_{O_2} regulation because the load disturbance is known, whereas, there is only an indirect measurement of λ_{O_2}. Feedforward control can accurately regulate λ_{O_2} to its desired value at the steady-state if all the model parameters are known. Specifically, feedforward control to air compressor voltage v_{cm}^{ff} can be applied based on the stack current I_{st} or the net current to the load, I_{net}, i.e. the compressor motor voltage is $v_{cm}^{ff} = f(I_{st}$ or $I_{net})$. The function $f(I_{st}$ or $I_{net})$ can be determined by the balance of oxygen mass consumed by the current and the compressor map from v_{cm} to W_{cp}. Also adding a feedforward controller may be helpful for this problem because the compressor voltage can be scheduled immediately after the current demand is issued, avoiding sensor or computational delays associated with any feedback compensation.

Regulating the oxygen supply to the cathode inlet is directly related with the current drawn from the stack; thus, feedforward control from the current measurement to the compressor motor command, I_{st} to v_{cm}^{ff}, is proposed in [12].

When the air supply compressor load is drawn from its own stack, the total stack current is the sum of the net current I_{net} and the compressor motor load current I_{cm}, which is calculated from the power consumption of the motor, P_{cm}. In small signal analysis, I_{cm} can be expressed through perturbation of (2) and (12) - (15)

$$\begin{aligned}\delta I_{cm} &= k_{v_{cm}}\delta v_{cm} - k_{\omega_{cp}}\delta\omega_{cp} - k_{v_{st}}\delta v_{st} \\ &= k_{v_{cm}}\delta v_{cm} - k_{\omega_{cp}}\delta\omega_{cp} + k_{v_{st,I_{st}}}\delta I_{st} - k_{v_{st,p}}\delta p_{O_2}\end{aligned} \tag{3}$$

where all k_is are positive constants calculated at the nominal operating point of 40 kW FC net power. Also it is assumed that v_{st} is a function of the stack current I_{st} and the oxygen partial pressure p_{O_2}. The effect of the nitrogen pressure or cathode pressure is assumed to be lumped into $k_{v_{st,p}}$ for simplicity. Here it is assumed that the electric drive for the compressor motor has a minimal energy buffer or filter; thus, compressor motor voltage command instantaneously adds the current load to the stack within the frequency range of interest in this work.

When the feedforward control is a function of the stack current given by $\delta v_{cm}^{ff} = k_{I_{st,ff}}\delta I_{st} = k_{I_{st,ff}}(\delta I_{net} + \delta I_{cm})$ and (3) ,

$$\begin{aligned}\delta v_{cm}^{ff} = \frac{k_{I_{st,ff}}}{1 - k_{I_{st,ff}}k_{v_{cm}}}(&\delta I_{net} - k_{\omega_{cp}}\delta\omega_{cp} \\ &+ k_{v_{st,I_{st}}}\delta I_{st} - k_{v_{st,p}}\delta p_{O_2})\end{aligned} \tag{4}$$

and the resulting stack current $\delta I_{st} = \delta I_{net} + \delta I_{cm}$, when the feedforward controller (4) is based on stack current, is

$$\begin{aligned}\delta I_{st} = \frac{1}{1 - k_{v_{st,I_{st}}} - k_{I_{st,ff}}k_{v_{cm}}}(&\delta I_{net} - k_{\omega_{cp}}\delta\omega_{cp} \\ &- k_{v_{st,p}}\delta p_{O_2}).\end{aligned} \tag{5}$$

If we assume a step change $I_{net,o}$ in net current from the nominal point $I_{net,n}$ ($\Delta I_{net}(s) = \frac{I_{net,o}}{s}$) drawn from the fuel cell with the above feedforward controller, the resulting initial value of the stack current I_{st} is

$$\begin{aligned}\delta I_{st}(0) &= \lim_{s\to\infty} s\Delta I_{st}(s) \\ &= \lim_{s\to\infty} s\left[\frac{1}{1 - k_{v_{st,I_{st}}} - k_{I_{st,ff}}k_{v_{cm}}}\Delta I_{net}(s)\right] \\ &= \frac{1}{1 - k_{v_{st,I_{st}}} - k_{I_{st,ff}}k_{v_{cm}}}I_{net,o} \\ &= 1.99 I_{net,o}\end{aligned} \tag{6}$$

since the initial deviations of $\delta\omega$ and δp_{O_2} from the steady-state value during the step net current are zero. Full lineariza-

[1]A 75 kW fuel cell stack is typically supplied by 15 kW compressor power [3], [11].

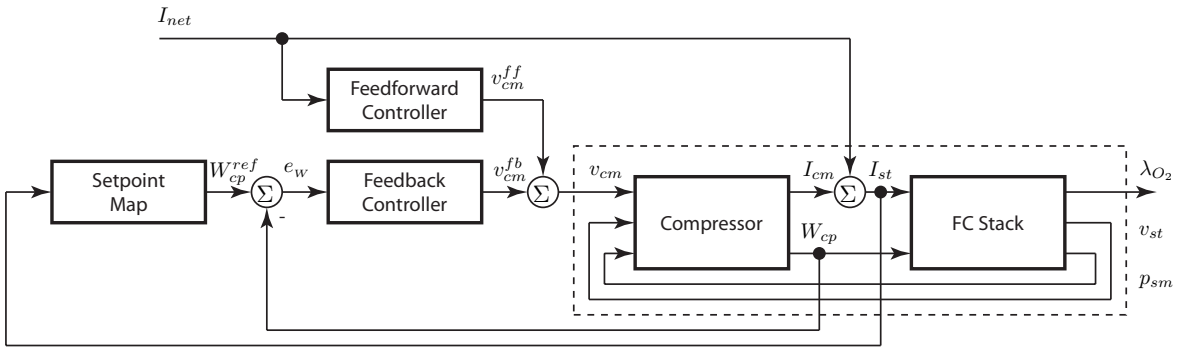

Fig. 2. Schematic of fuel cell with air flow control using compressor

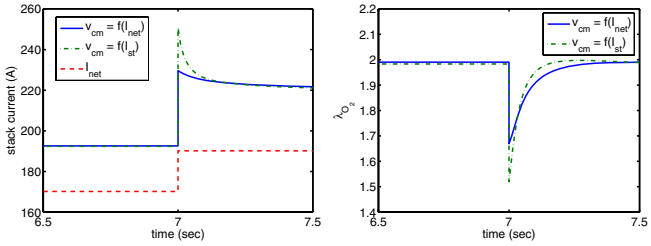

(a) Stack current (b) Oxygen excess ratio

Fig. 3. Feedforward control comparison

tion using the linmod command in MATLAB® [2]is also used to confirm that the initial value from unit step I_{net} to I_{st} becomes 1.90, while the steady state stack current is 1.33 from the final value or DC gain.

Another way of constructing feedforward control, which is suggested in [2], is based on the net current I_{net} measurement, which replaces I_{st}. The net current is smaller than the amount of the entire stack current, but it can still capture the stack current dynamics and has the ability to regulate λ_{O_2} in the steady state.

Similar calculations with (5) in the case when $\delta v_{cm}^{ff} = k_{I_{net,ff}} \delta I_{net}$ show that

$$\delta I_{st} = \frac{1 + k_{v_{cm}} k_{I_{net,ff}}}{1 - k_{v_{st,I_{st}}}} \delta I_{net} - \frac{k_{\omega_{cp}}}{1 - k_{v_{st,I_{st}}}} \delta \omega_{cp} - \frac{k_{v_{st,p}}}{1 - k_{v_{st,I_{st}}}} \delta p_{O_2}. \quad (7)$$

The initial value of the stack current I_{st} with respect to a step net current is approximately

$$\delta I_{st}(0) = \frac{1 + k_{v_{cm}} k_{I_{net,ff}}}{1 - k_{v_{st,I_{st}}}} I_{net,o} = 1.70 I_{net,o} \quad (8)$$

which is also confirmed numerically using MATLAB®. The numerical value of initial stack current versus unit net current input is 1.68, which is smaller than the initial stack current observed when the feedforward depends on the total stack current.

[2]MATLAB is registered trademark of The MathWorks, Inc.

Fig. 3 depicts a simulation comparison between stack current feedforward and net current feedforward control. Both static controllers are designed to achieve $\lambda_{O_2} = 2$ in the steady state with different maps from I_{st} or I_{net} to v_{cm}^{ff}. Although both feedforward controllers achieve oxygen excess ratio regulation in the steady state, there are differences in transient performance when a step net current of 20 A is drawn, corresponding to a power step from 40 to 45 kW. As can be seen in Fig. 3(a), the I_{st}-based feedforward control generates a larger peak in the entire stack current than in I_{net}-based feedforward control. The current increment resulting from the subsequent compressor work adds another current load leading to a positive feedback loop. The actual initial peak of the stack current in the case of I_{st} feedforward control is greater than the expected amount from the linearized model because the compressor motor current I_{cm} exhibits nonlinear behavior as the stack current increases. Increase in stack current directly degrades λ_{O_2} producing a large excursion before sufficient oxygen is supplied to the cathode (Fig. 3(b)). On the other hand, λ_{O_2} recovers faster in I_{st} feedforward case because the compressor is forced to blow more air at the initial transient with larger I_{st}. The time constant of λ_{O_2} recovery depends on the eigenvalues of the system including feedforward controller, $s = -3.12, -3.91, -23.3, -71.4$. The I_{net}-based feedforward control recovers λ_{O_2} slower than the stack current feedforward associated with the slightly slower eigenvalues, $s = -3.12, -3.29, -19.7, -71.3$.

IV. Feedback Control Limitation

To improve the steady-state λ_{O_2} regulation despite modeling errors or device aging, a feedforward controller v_{cm}^{ff} can be combined with the feedback controller based on the compressor flow measurement W_{cp} (shown in Fig. 2). The setpoint map in Fig. 2 determines the demanded air flow rate W_{cp}^{ref} for the flow rate measurement position based on the measured stack current I_{st} and the desired oxygen excess ratio $\lambda_{O_2}^{ref}$, as defined in [12] Eq. (27). Note here that the reference flow $W_{cp}^{ref}(I_{st}, \lambda_{O_2}^{ref})$ must be calculated to support the stack load (I_{st}) and not I_{net} for steady-state λ_{O_2} regulation. Then feedback control formulation can be

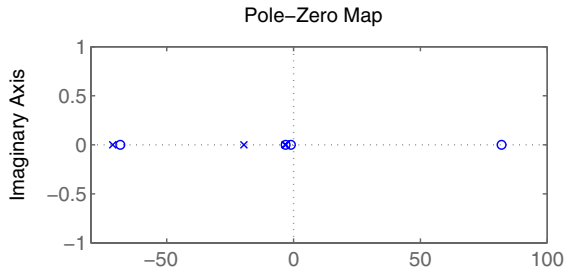

Fig. 4. The location of poles and zeros

applied to minimize the error between W_{cp}^{ref} and W_{cp}

$$e_W = W_{cp}^{ref} - W_{cp} \tag{9}$$

using compressor command v_{cm} as shown in Fig. 2 and proposed in [2].

Fig. 4 depicts the location of poles and zeros in the compressor control (v_{cm}) to error output (e_W) transfer function. It can be seen that there exists a right-half-plane zero at $s = 82.07$. The feedback controller from e_W to v_{cm} needs to be tuned judiciously due to non-minimum phase (NMP) zero in the open loop plant from v_{cm} to e_W. The non-minimum phase behavior in fuel cell dynamics is first introduced in [9], but only referred to the input/output pair, compressor motor voltage (v_{cm}) to net power (P_{net}). The variable P_{net} is neither directly measured nor used for feedback in a vehicle application and thus the NMP dynamics identified in [9] do not impose any control limitations. The NMP behavior from v_{cm} to e_W imposes bandwidth limitation [13] on the ability of air flow W_{cp} to track flow requirement $W_{cp}^{ref}(I_{st})$, which is empirically observed in [2].

V. Feedback Control Design

A feedback controller design will be performed based on the following facts: (i) fast closed-loop bandwidth for regulating compressor airflow W_{cp} does not guarantee the bandwidth of performance output λ_{O_2}; (ii) there exists feedback bandwidth limitation due to the NMP zero at $s = 82.07$; (iii) baseline results for the controller design should be those with I_{net}-based feedforward controller, because high frequency control effort in air supply compressor degrades λ_{O_2} regulation. Thus feedback control is tuned to only minimize steady state error.

A proportional and integral (PI) controller can be applied to the difference of W_{cp} and W_{cp}^{ref}. The voltage control command can be written as

$$\begin{aligned} v_{cm}(t) &= v_{cm}^{ff}(t) + v_{cm}^{fb}(t) \\ &= f(I_{net}) + K_P\left(W_{cp}^{ref}(I_{st}(t)) - W_{cp}(t)\right) \\ &\quad + K_I \int_0^t \left(W_{cp}^{ref}(I_{st}(\tau)) - W_{cp}(\tau)\right) d\tau. \end{aligned} \tag{10}$$

Fig. 5 shows the performance for feedforward and feedback+feedforward control. During a step input of net current I_{net}, the oxygen excess ratio initially drops because the additional air flow that can compensate the amount of increased

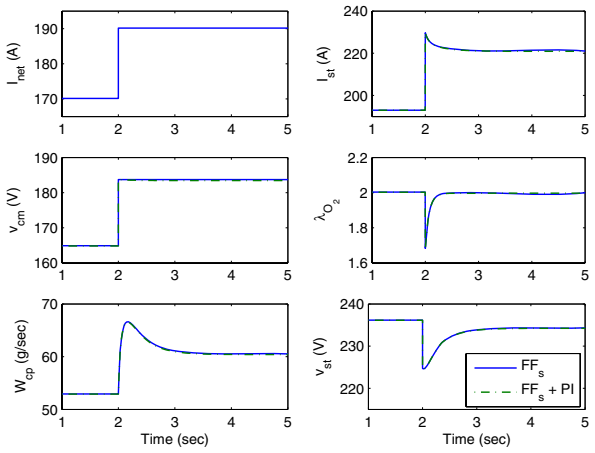

Fig. 5. Closed-loop fuel cell simulation

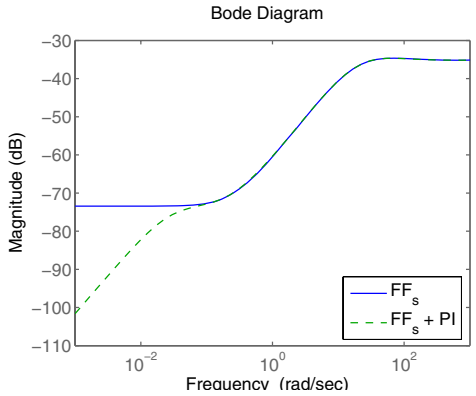

Fig. 6. Frequency response of the closed-loop fuel cell system - from I_{net} to λ_{O_2}

current has not yet reached the cathode. The oxygen excess ratio λ_{O_2} recovers quickly due to the feedforward control and settles to the desired steady-state value with no error due to the PI controller. Frequency responses in Fig. 6 show the differences when adding feedback control. The feedback controller with very slow bandwidth (< 0.1 rad/s) rejects the low-frequency disturbance inputs, without increasing control effort at frequencies where it is actually harmful to λ_{O_2} regulation.

Apart from the stability considerations in the PI gain tuning, high frequency v_{cm} commands (> 100 rad/s) should be avoided. The effect of high frequency control signals can be explained more clearly in the frequency domain. Fig. 7 shows the frequency response from compressor motor command v_{cm} to measurement W_{cp} and performance output λ_{O_2}. As can be seen in the figure, v_{cm} contributes to λ_{O_2} in the opposite direction after 100 rad/s, while effects of v_{cm} to compressor airflow W_{cp} naturally roll off at high frequency. This demonstrates that high frequency compressor command increases only the stack current but does not necessarily help in supplying air to the cathode. Finally the PI gain is determined in a way not to deteriorate the performance in high frequency (> 100 rad/s) and achieve zero steady-state.

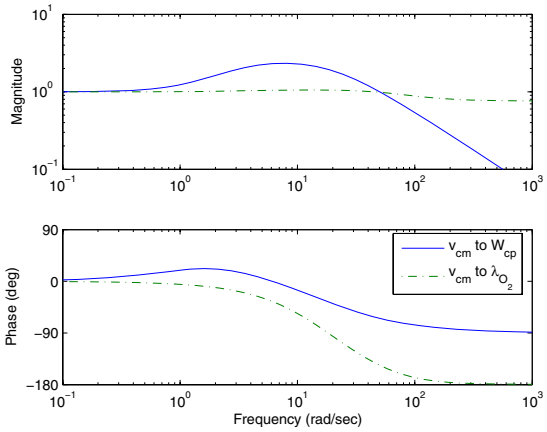

Fig. 7. Frequency response from control to outputs

Thus, the difficulty and control limitations are more pronounced in the case where the compressor is powered directly by the fuel cell and not an auxiliary power unit. In fact the limitation in controlling oxygen starvation becomes more severe from the compressor and fuel cell electric coupling and not from the manifold filing dynamics as frequently quoted in literature [3], [4], [11], [14]. Indeed, when the compressor power is drawn directly from the fuel cell, there is a direct conflict between regulating the compressor air mass flow and regulating the oxygen excess ratio. Fast air flow control requires large compressor power that increases the current drawn from the stack. This direct coupling between the actuator signal v_{cm} and the performance variable λ_{O_2} especially at high frequencies exacerbates the difficulties in controlling the air flow to the fuel cell during step increase in load.

VI. Conclusion

Control design limitations of a power-autonomous fuel cell system are discussed in this paper. A low-order FC system model has been introduced to describe the flow and power dynamics using physical principles and stack polarization. The inertial dynamics of the compressor, manifold filling dynamics and partial pressures are captured.

Different feedforward architectures were considered and analyzed. The coupling between the power and flow paths through in a compressor driven fuel cell stack is clarified. This coupling imposes control limitations manifested through a NMP-zero in the air flow control path.

Appendix I
Fuel Cell System Model

We consider a fuel cell stack with active cell area of A_{fc} = 280 cm^2 and $n = 381$ number of cells with 75 kW gross power output that is applicable for automotive and residential use. The performance variables for the FC power system are (i) the stack voltage v_{st} that directly influences the stack power generated $P_{fc} = v_{st}I_{st}$ when the load (current) I_{st} is drawn from the stack, and (ii) the oxygen excess ratio λ_{O_2} in

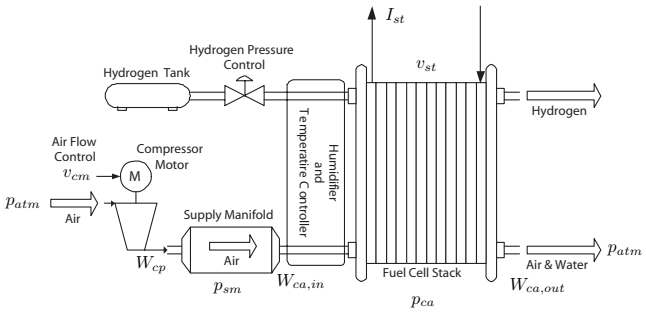

Fig. 8. Fuel cell reactants supply system

the cathode that indirectly ensures adequate oxygen supply to the stack.

Stack voltage is calculated as the product of the number of cells and cell voltage $v_{st} = nv_{fc}$. The combined effect of thermodynamics, kinetics, and ohmic resistance determines the output voltage of the cell

$$v_{fc} = E - v_{act} - v_{ohm} - v_{conc} \tag{11}$$

where E is the open circuit voltage, v_{act} is the activation loss, v_{ohm} is the ohmic loss, and v_{conc} is the concentration loss. The detailed equation of the FC voltage, also known as, polarization characteristic can be found in [3]. Depending on the load (current) drawn from the fuel cell and the air supply to the fuel cell, the stack voltage varies between 220 V to 350 V.

The FC voltage is given as static function of current density $i_{fc} = I_{st}/A_{fc}$ and several other variables such as oxygen and hydrogen partial pressures p_{O_2} and p_{H_2}, cathode pressure p_{ca}, temperature T_{st} and humidity λ_m. Although we assume instantaneous electrochemical reaction and negligible electrode double layer capacity, the FC voltage has a rich dynamic behavior due to its dependance on dynamically varying stack variables $(i_{fc}, p_{O_2}, p_{ca}, p_{H_2}, T_{st}, \lambda_m)$. We assume a compressed hydrogen supply as shown in Fig. 8 that simplifies the control of anode reactant flow. The cooler and humidifier are neglected for this work because their power requirement are smaller than the compressor power [15].

The dynamic behavior of the variables associated with the air flow control, namely, oxygen pressure p_{O_2}, total cathode pressure p_{ca}, and oxygen excess ratio in the cathode λ_{O_2} can be found in [3], [9]. The flow dynamics of the oxygen and hydrogen reactants are governed by pressure dynamics through flow channels, manifolds, orifices.

The mass continuity of the oxygen and nitrogen inside the cathode volume and ideal gas law yield

$$\frac{dp_{O_2}}{dt} = \frac{\bar{R}T_{st}}{M_{O_2}V_{ca}}\left(W_{O_2,in} - W_{O_2,out} - W_{O_2,rct}\right), \tag{12}$$

$$\frac{dp_{N_2}}{dt} = \frac{\bar{R}T_{st}}{M_{N_2}V_{ca}}\left(W_{N_2,in} - W_{N_2,out}\right) \tag{13}$$

where V_{ca} is the lumped volume of cathode, $\bar{R}$ is the universal gas constant, and M_{O_2} and M_{N_2} are the molar mass of oxygen and nitrogen, respectively.

The compressor motor state is associated with the rotational dynamics of the motor through thermodynamic equations. A lumped rotational inertia is used to describe the compressor with the compressor rotational speed ω_{cp}

$$\frac{d\omega_{cp}}{dt} = \frac{1}{J_{cp}}\left(\tau_{cm} - \tau_{cp}\right) \tag{14}$$

where τ_{cm} is the compressor motor torque and τ_{cp} is the load torque of the compressor.

The rate of change of air pressure in the supply manifold that connects the compressor with the fuel cell (shown in Fig. 8) depends on the compressor flow into the supply manifold W_{cp}, the flow out of the supply manifold into the cathode $W_{ca,in}$ and the compressor flow temperature T_{cp}

$$\frac{dp_{sm}}{dt} = \frac{\bar{R}T_{cp}}{M_{a,atm}V_{sm}}\left(W_{cp} - W_{ca,in}\right) \tag{15}$$

where V_{sm} is the supply manifold volume and $M_{a,atm}$ is the molar mass of atmospheric air.

The inlet mass flow rate of oxygen $W_{_{O_2},in}$ and nitrogen $W_{_{N_2},in}$ can be calculated from the inlet cathode flow $W_{ca,in}$ as follows

$$W_{_{O_2},in} = \frac{x_{_{O_2},atm}}{1+w_{atm}}W_{ca,in}, W_{_{N_2},in} = \frac{1-x_{_{O_2},atm}}{1+w_{atm}}W_{ca,in} \tag{16}$$

where $x_{_{O_2},atm}$ is the oxygen mass fraction of the inlet air associated with the oxygen molar ratio $y_{_{O_2},atm} = 0.21$ and w_{atm} is the humidity ratio of inlet air.

The supply manifold model describes the mass flow rate from the compressor to the outlet mass flow. A linear flow-pressure condition $W_{ca,in} = k_{ca,in}(p_{sm} - p_{ca})$ is assumed due to the small pressure difference between the supply manifold p_{sm} and the cathode pressure p_{ca} which is the sum of oxygen, nitrogen and vapor partial pressures $p_{ca} = p_{_{O_2}} + p_{_{N_2}} + p_{sat}$ with the vapor saturation pressure $p_{sat} = p_{sat}(T_{st})$. The total flow rate at the cathode exit $W_{ca,out}$ is calculated by the nozzle flow equation because the pressure difference between the cathode and the ambient pressure is large in pressurized stacks.

The rate of oxygen consumption $W_{_{O_2},rct} = M_{_{O_2}}\frac{nI_{st}}{4F}$ in (12) depends on the stack current I_{st} and the Faraday number F. The oxygen excess ratio

$$\lambda_{_{O_2}} = \frac{W_{_{O_2},in}}{W_{_{O_2},rct}} \tag{17}$$

is typically regulated at $\lambda_{_{O_2}}^{ref} = 2$ to reduce the formation of stagnant vapor and nitrogen films in the electrochemical area. Values of $\lambda_{_{O_2}}$ lower than 1 indicate oxygen starvation and has serious consequences in the stack life.

The compressor motor torque $\tau_{cm} = P_{cm}/\omega_{cp}$ depends on the power

$$P_{cm} = v_{cm}(v_{cm} - k_v\omega_{cp})/R_{cm} \tag{18}$$

provided by the compressor motor, which is calculated using the compressor motor voltage input v_{cm} and its rotational speed ω_{cp}. In this paper, the compressor power is supplied directly from the fuel cell instead of a secondary battery, establishing a power-autonomous fuel cell system (Fig. 1).

REFERENCES

[1] Y. Motozono, M. Yamashita, M. Yamaoka, K. Nagamiya, and I. Maeda, "Fuel cell control apparatus," U.S. Patent 6 638 652, Oct. 28, 2003.

[2] W. Mufford and D. Strasky, "Power control system for a fuel cell powered vehicle," U.S. Patent 5 991 670, Nov. 23, 1999.

[3] J. T. Pukrushpan, H. Peng, and A. G. Stefanopoulou, "Control-oriented modeling and analysis for automotive fuel cell systems," *ASME J. Dyn. Syst., Meas., Control*, vol. 126, no. 1, pp. 14–25, 2004.

[4] P. Rodatz, G. Paganelli, and L. Guzzella, "Optimizing air supply control of a PEM fuel cell system," in *Proc. Amer. Control Conf.*, vol. 3, Denver, CO, June 2003, pp. 2043–2048.

[5] S. D. Knights, K. M. Colbow, J. St-Pierre, and D. P. Wilkinson, "Aging mechanisms and lifetime of PEFC and DMFC," *Journal of Power Sources*, vol. 127, pp. 127–134, 2004.

[6] J. St-Pierre, D. P. Wilkinson, S. Knights, and M. Bos, "Relationships between water management, contamination and lifetime degradation in PEFC," *Journal of New materials for Electrochemical Systems*, vol. 3, pp. 99–106, 2000.

[7] J. M. Cunningham, M. A. Hoffman, and D. J. Friedman, "A comparison of high-pressure and low-pressure operation of PEM fuel cell systems," SAE paper 2001-01-0538, 2001.

[8] S. Gelfi, A. G. Stefanopoulou, J. T. Pukrushpan, and H. Peng, "Dynamics of lower-pressure and high-pressure fuel cell air supply systems," in *Proc. Amer. Control Conf.*, vol. 3, Denver, CO, June 2003, pp. 2049–2054.

[9] J. T. Pukrushpan, A. G. Stefanopoulou, and H. Peng, *Control of Fuel Cell Power Systems: Principles, Modeling, Anylysis and Feedback Design*, ser. Advances in Industrial Control. London: Springer-Verlag Telos, 2004.

[10] G. Boehm, D. P. Wilkinson, S. Khight, R. Schamm, and N. J. Fletcher, "Method and appratus for operating a fuel cell," U.S. Patent 6 461 751, Oct. 8, 2002.

[11] J. M. Cunningham, M. A. Hoffman, R. M. Moore, and D. J. Friedman, "Requirements for a flexible and realistic air supply model for incorporation into a fuel cell vehicle (FCV) system simulation," SAE paper 1999-01-2912, 1999.

[12] J. T. Pukrushpan, A. G. Stefanopoulou, and H. Peng, "Control of fuel cell breathing," *IEEE Control Syst. Mag.*, vol. 24, no. 2, pp. 30–46, Apr. 2004.

[13] J. S. Freudenberg, "A first graduate course in feedback control," EECS 565 Coursepack, University of Michigan, 2004.

[14] J. Sun and I. Kolmanovsky, "Load governor for fuel cell oxygen starvation protection: A robust nonlinear reference governor approach," in *Proc. Amer. Control Conf.*, vol. 1, Boston, MA, June 2004, pp. 828–833.

[15] D. D. Boettner, G. Paganelli, Y. G. Guezennec, G. Rizzoni, and M. J. Moran, "Proton exchange membrane fuel cell system model for automotive vehicle simulation and control," *ASME Journal of Energy Resources Technology*, vol. 124, pp. 20–27, 2002.